Stability analysis of the Labrador Current

ASOF meeting, AWI Bremerhaven
16.03.2015
by Sören Thomsen

GEOMAR
Helmholtz-Zentrum für Ozeanforschung Kiel

Carsten Eden and Lars Czeschel

KlimaCampus

Universität Hamburg
DER FORSCHUNG | DER LEHRE | DER BILDUNG

Outline

1) Motivation
   -> Labrador Current
   -> seasonality of EKE along the Labrador Current

2) FLAME model

3) Linear stability analysis

3) Results
   -> interior mode
   -> oceanic background conditions

4) Discussion

5) Summary and conclusion

Labrador Current

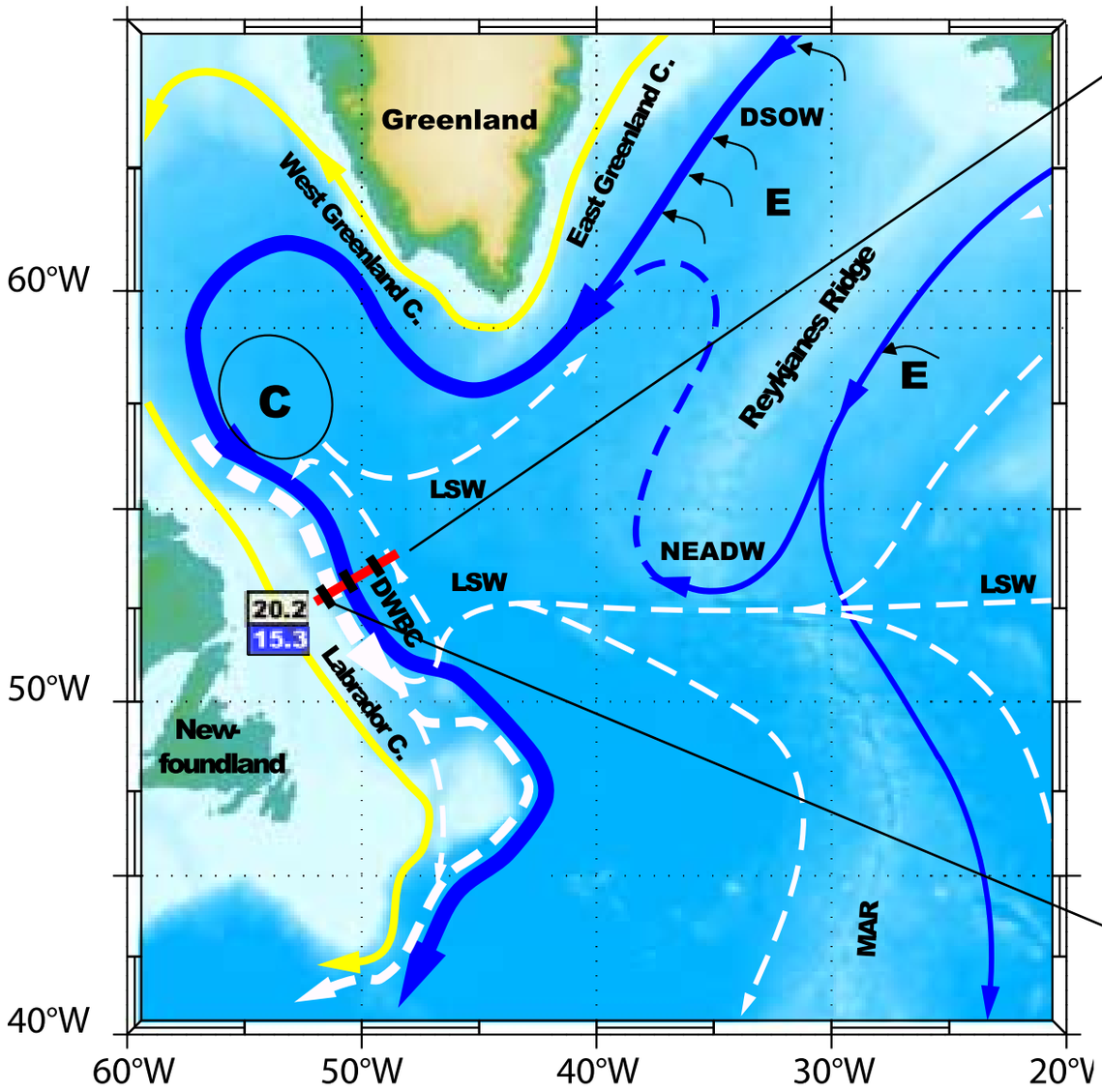

Fischer et al. 2010

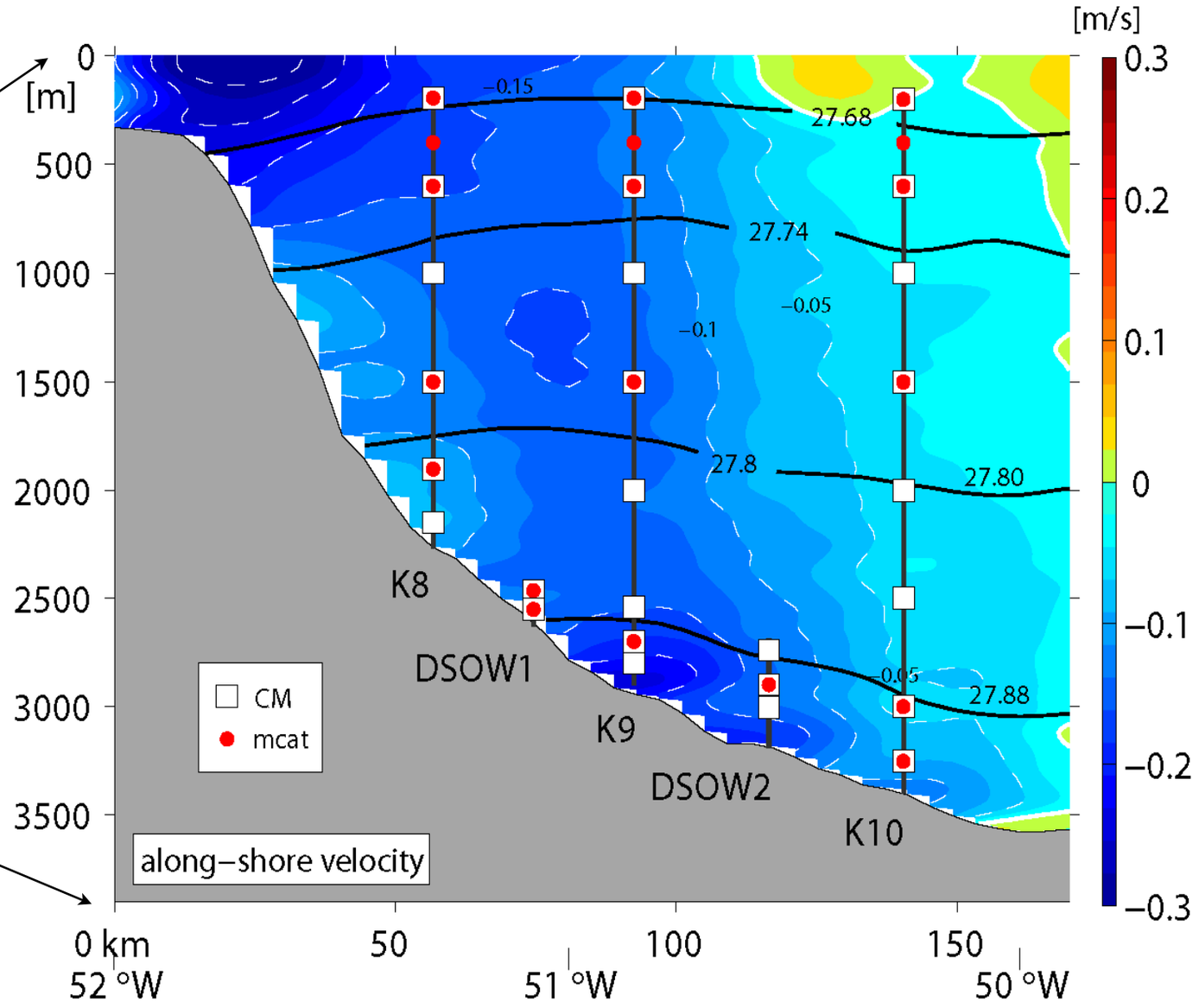

Fischer et al. 2014

LSW transformation and export

Jan/Mar LSW thickness change

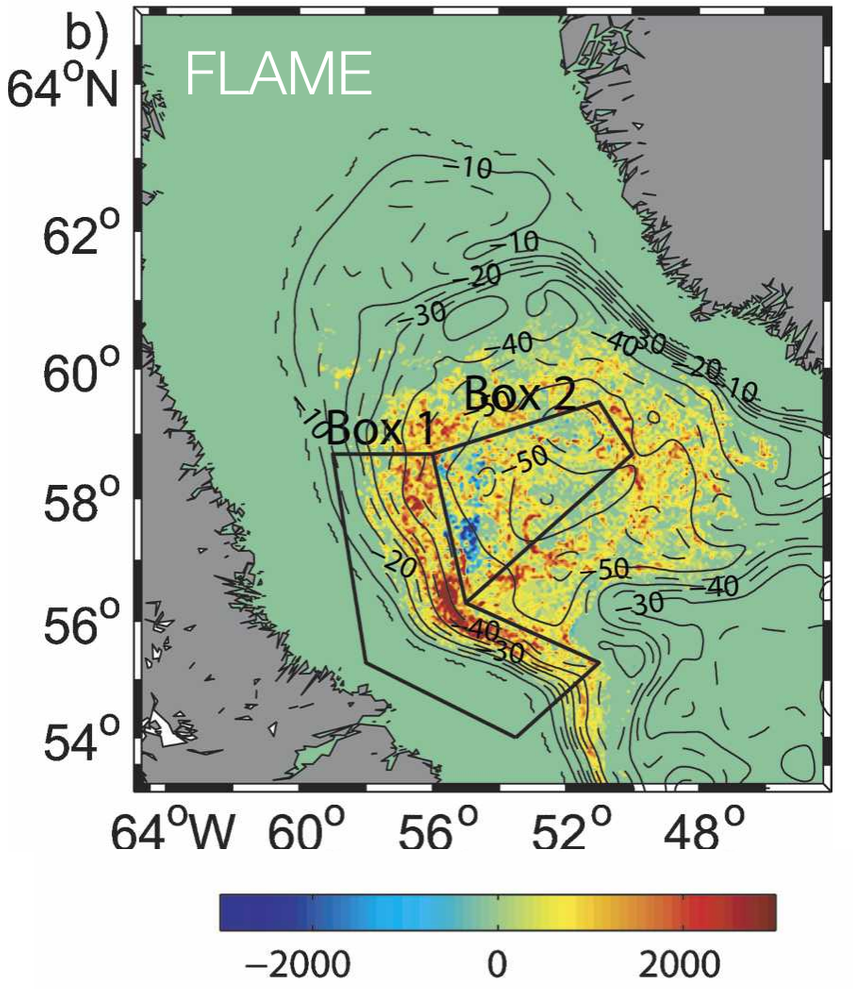

Brandt et al. 2007

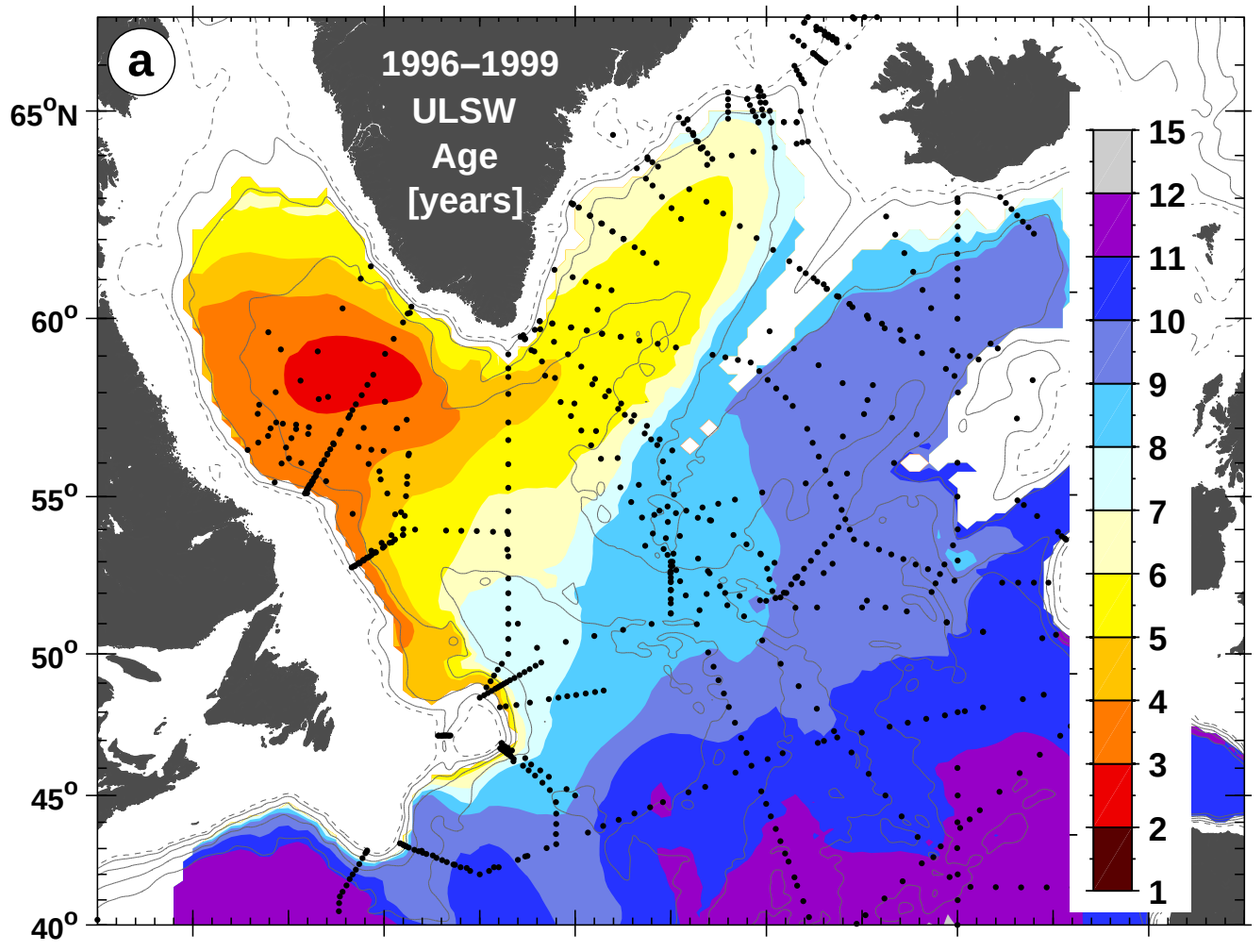

Rhein et al. 2015

-> Labrador Current is important water mass transformation area
(Pickart et al. 1997, 2002, Spall and Pickart 2001, Straneo et al. 2002, Cuny et al. 2005, Pickart and Spall 2007, Brandt et al. 2007, Spall 2010)

-> rapid export of ULSW into subtropical gyre
(Schott et al. 2004, Brandt et al. 2007, Rhein et al. 2015)

Seasonality of EKE along LC

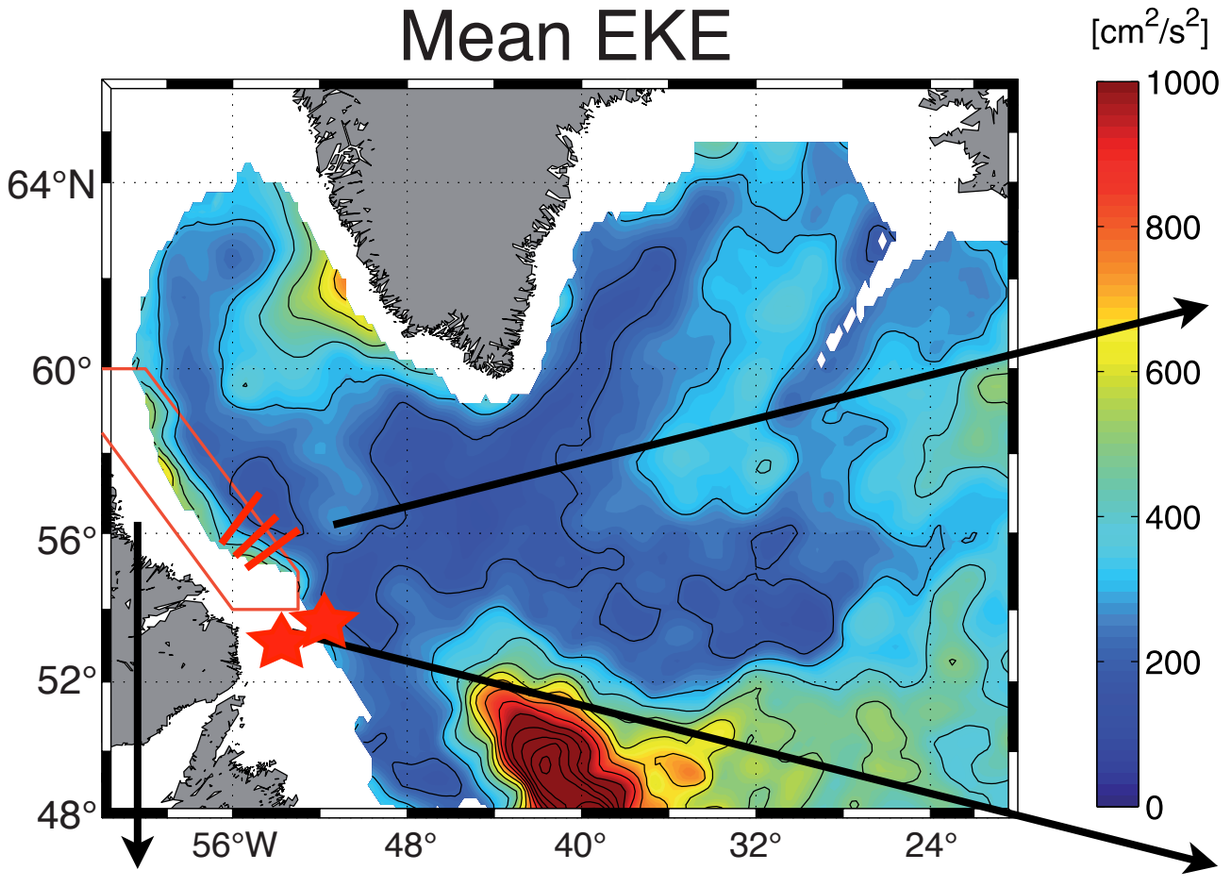

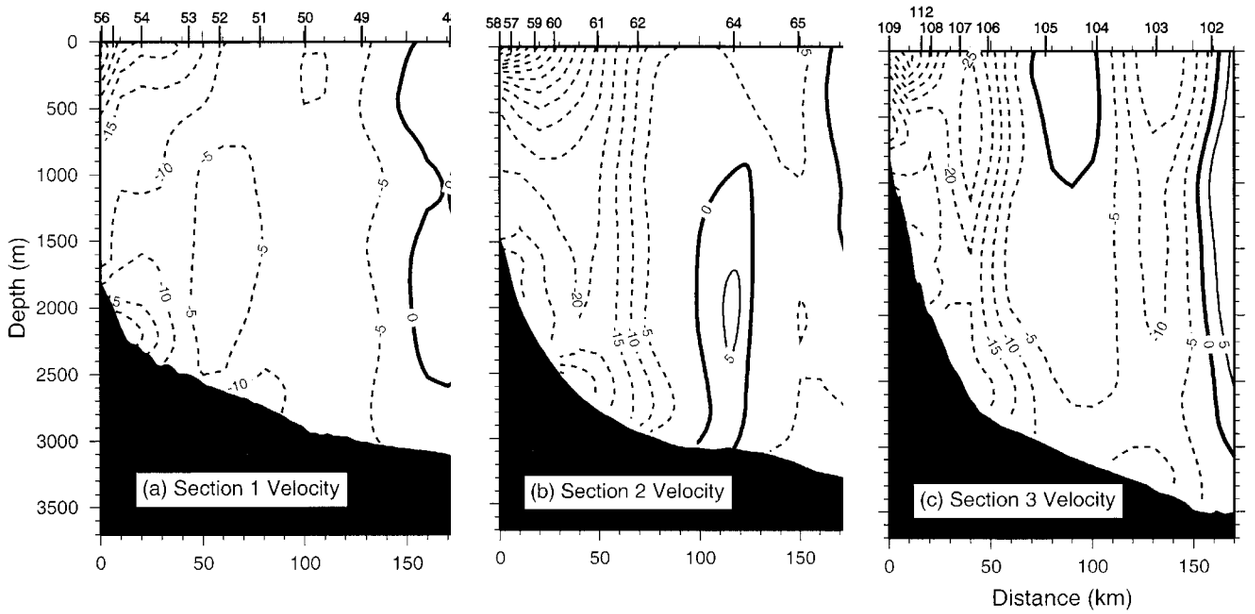

Pickart et al. 2002

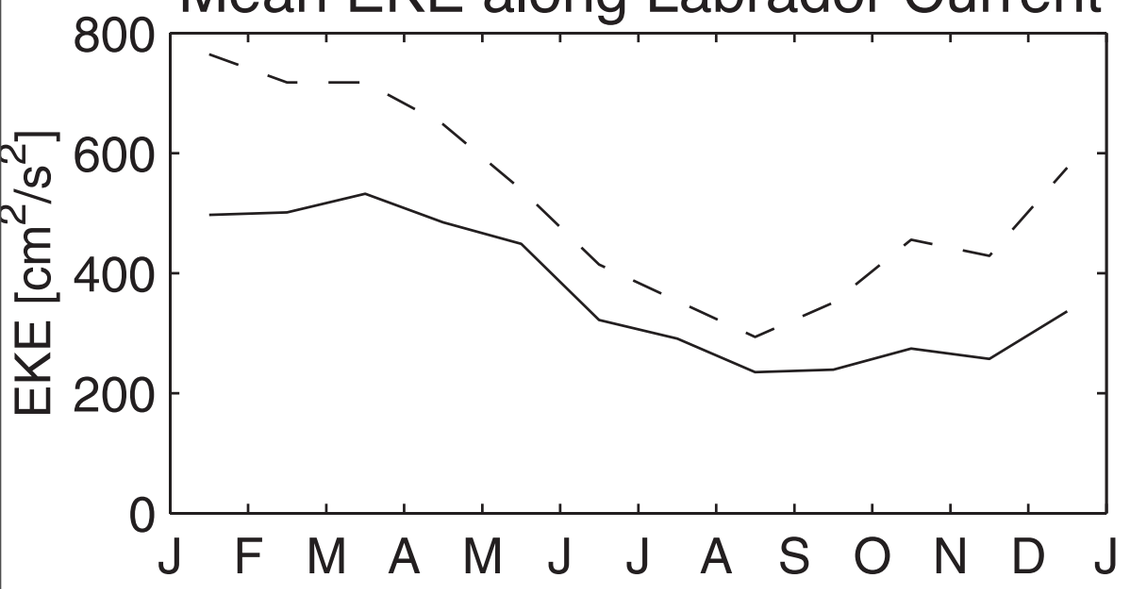

Brandt et al. 2004

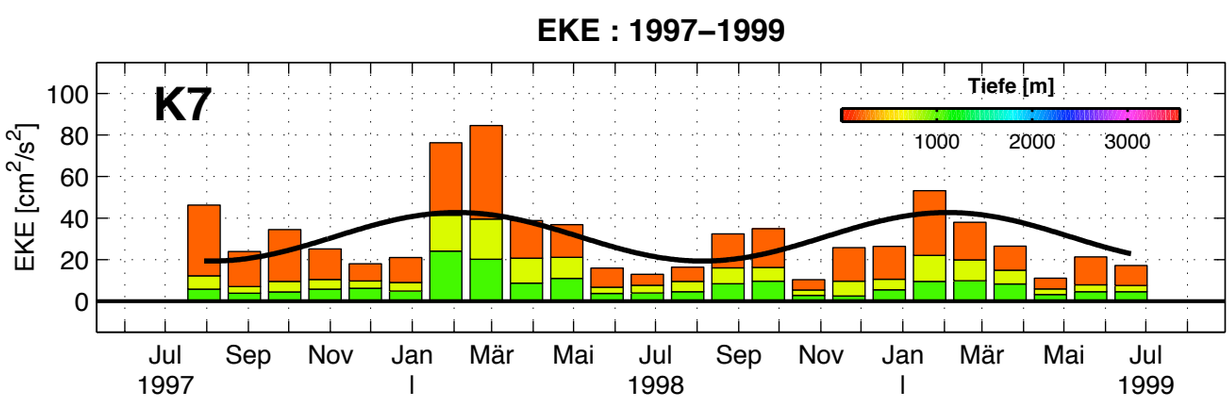

Morsdorf 2001 (Dipl. Thesis)

Research questions

1) Why does the **Labrador Current** become unstable in **late winter** and what kind of **instability** is at work?

2) How do the **oceanic background conditions** contribute?

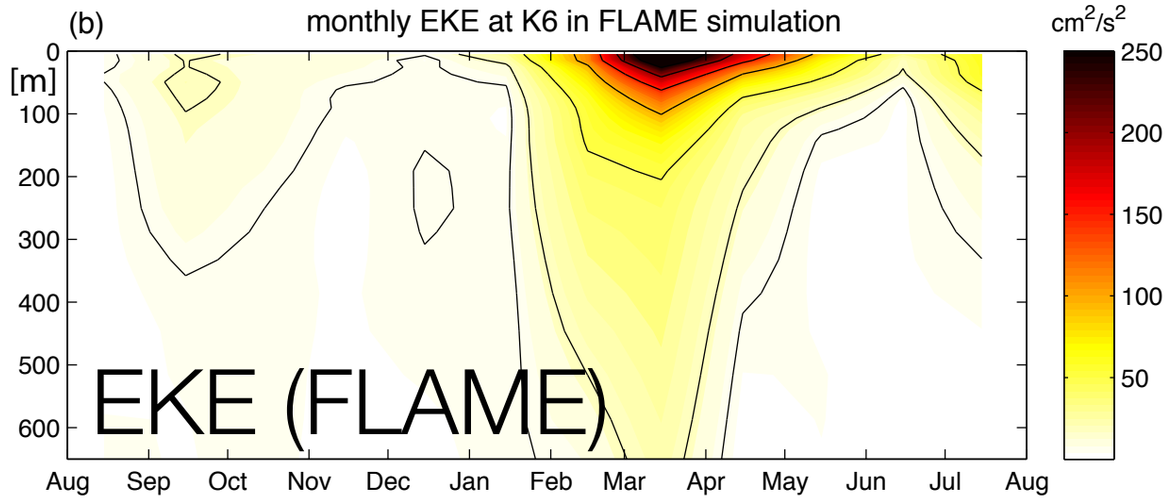

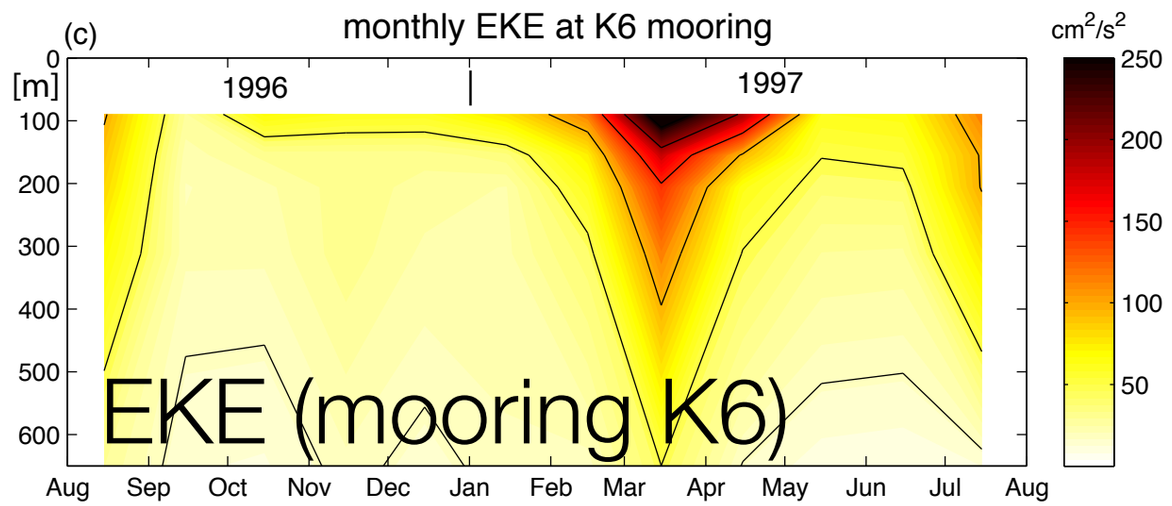

Data / Model / Method

- **moored current data** in Labrador Current (K6, K7, K8 see Fischer et al. 2004, Cuny et al. 2005)

- **1/12°** north Atlantic ocean model from the Family of Linked Atlantic Model Experiments (**FLAME**)

- non-geostrophic **linear stability analysis** to investigate the stability problem

FLAME Model

- 1/12° -> dx = 4 - 5 km
- 45 non-equidistant vertical levels
- primitive equations, hydrostatic
- forcing: clim. monthly mean wind and surface fluxes

- Czeschel (PhD 2005) improved hydrography and deep convection

-> realistic mixed layer depths

- Brandt et al. (2007) studied transformation and export of Labrador Sea Water

mixed layer depth March

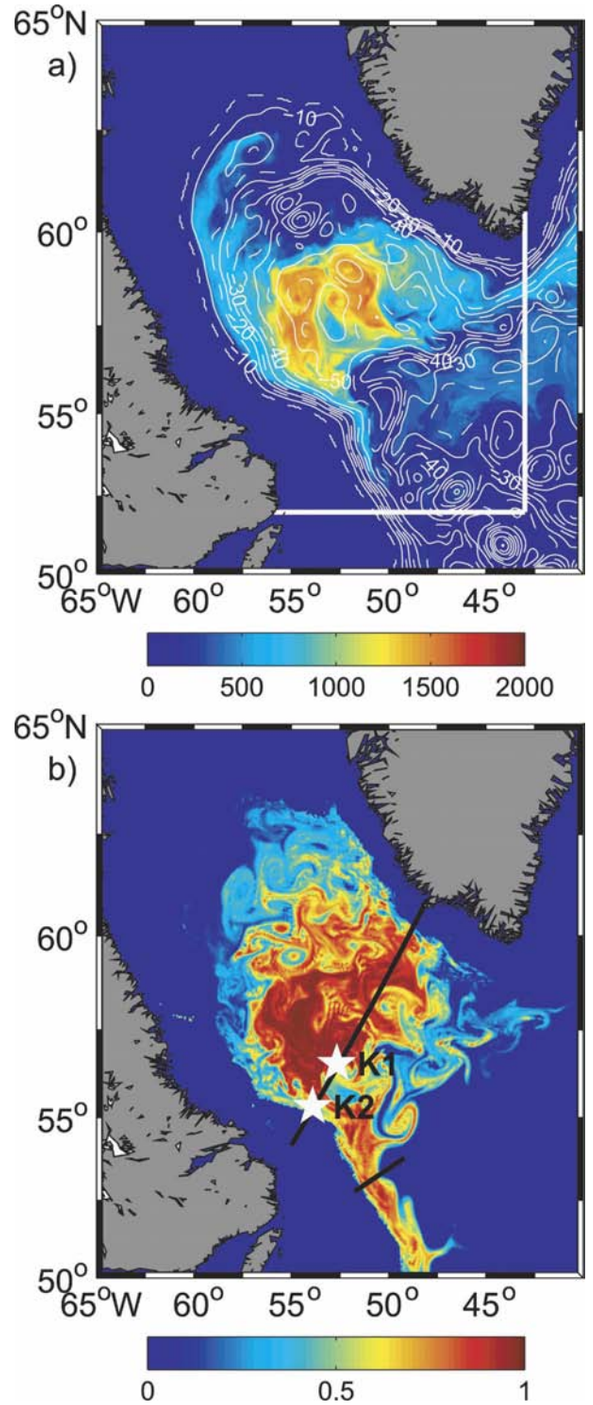

FIG. 1. (a) Simulated mixed layer depth (m; color shading) superimposed on barotropic streamfunction (Sv; isolines) during March and (b) concentration of the idealized ventilation tracer in the σ_θ range 27.77–27.80 kg m^{-3} during May; (a) also shows the chosen limits for the Labrador Sea region, i.e., the 52°N and the 43°W section, and (b) shows the LC section at about 53°N and the WOCE AR7W section running across the deep Labrador Sea, as well as the locations of moorings K1 and K2 (white stars).

Brandt et al. 2007

Unstable Labrador Current

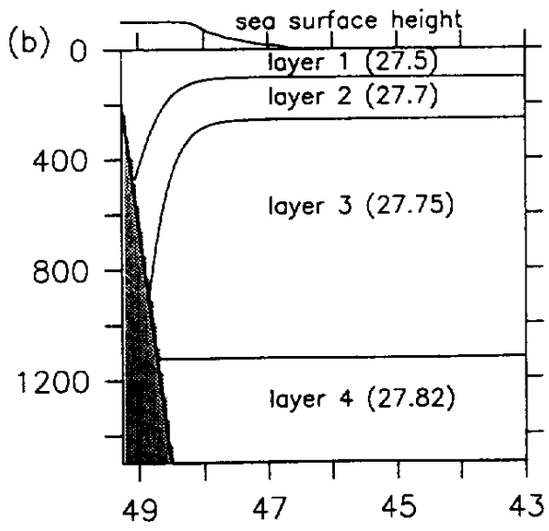

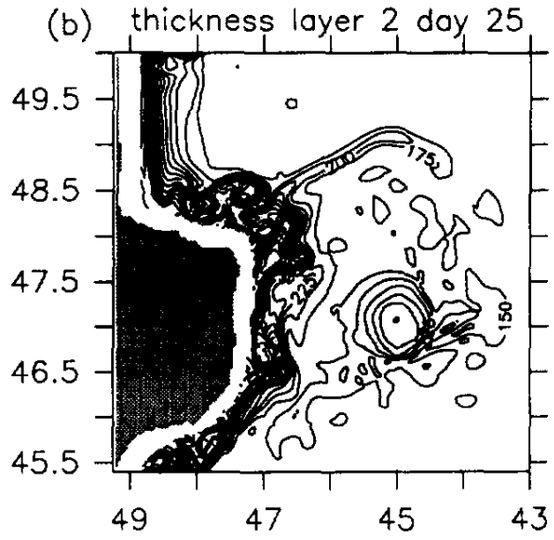

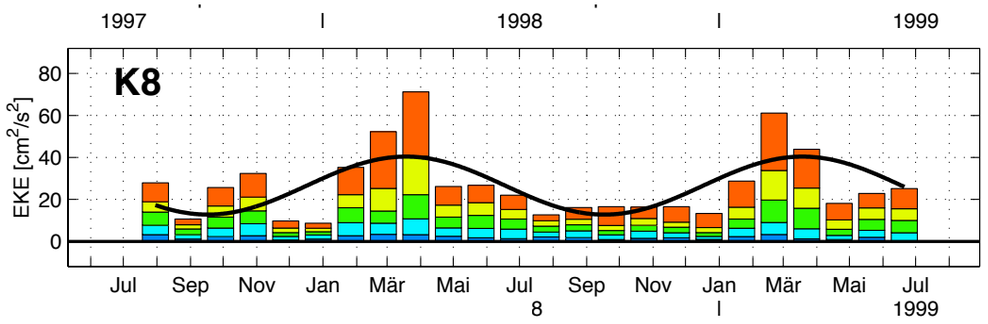

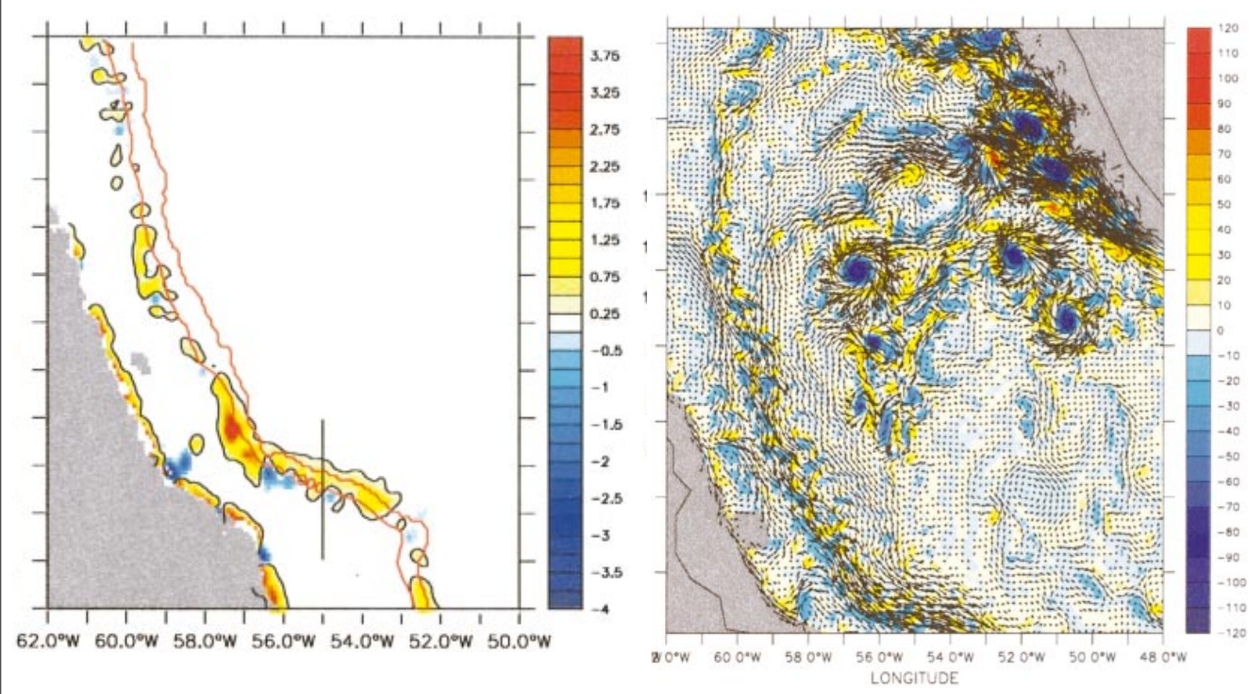

- Pickart et al. 1997 studied uLSW eddy formation process in four-layer primitive equation model

- EKE due to high frequency wind forcing? (Morsdorf, 2001)

- monthly mean winds to exclude high-frequency winds as a direct source of EKE (Eden and Böning, 2002)

- baroclinic >> barotropic transfer terms (Eden and Böning, 2002)

-> focus on baroclinic instability problem

Baroclinic instability

- **growth rate** of baroclinic waves

- larger growth rates -> more **unstable** waves

- **growth rate** depends on **Richardson number** (Eady 1949)

- **non-geostrophic** baroclinic instability problem (Stone 1966, 1970, 1971,1972)

- **growth rate** correlates with **EKE** (Stammer, 1997, Chelton et al. 2007)

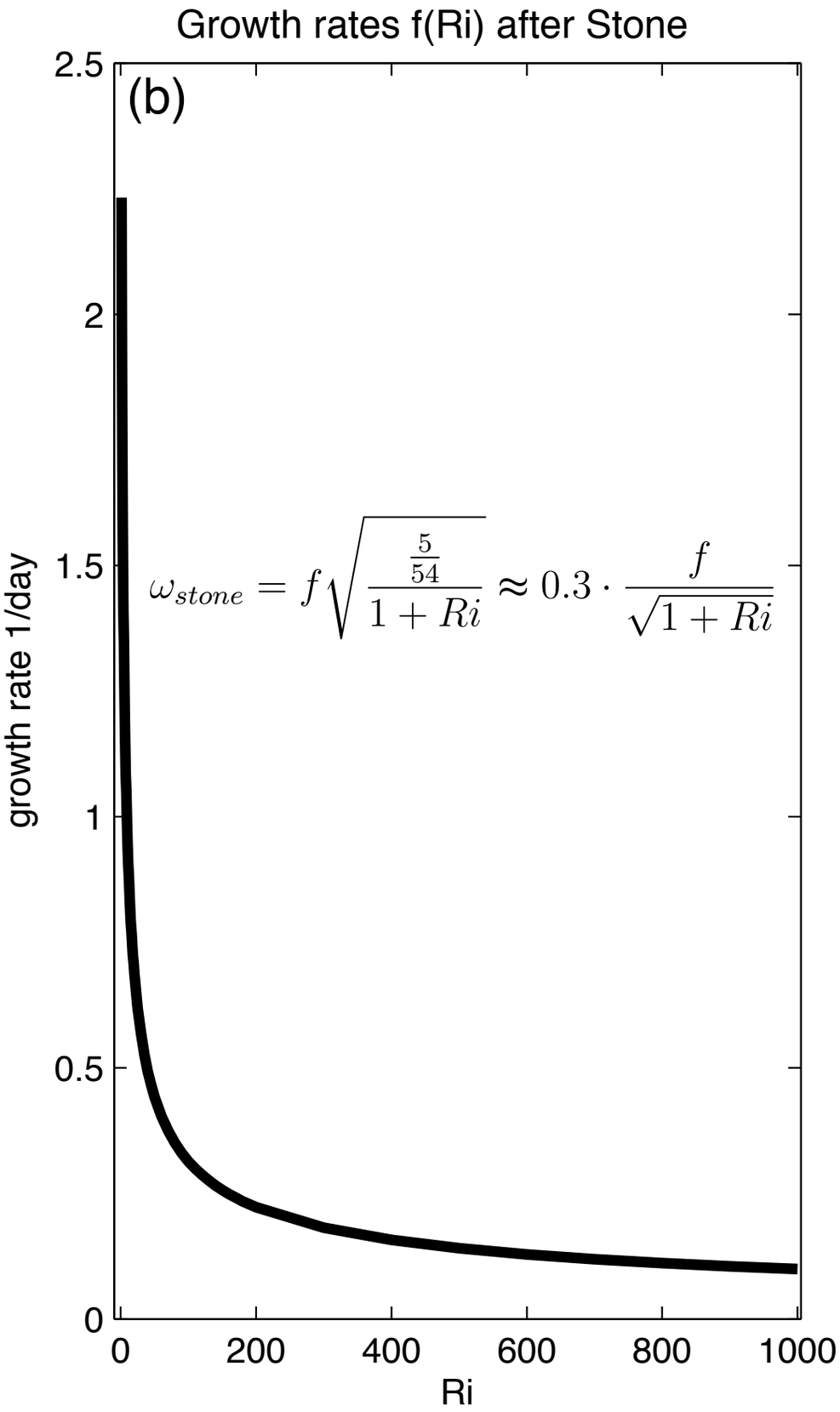

Non-geostrophic linear stability analysis

Set of equations:

$$
\begin{aligned}
\partial_t u + \boldsymbol{u}\cdot\boldsymbol{\nabla} u - fv + f_h w &= -\partial_x p && \text{momentum}\\
\partial_t v + \boldsymbol{u}\cdot\boldsymbol{\nabla} v + fu &= -\partial_y p &&\\
\partial_t w + \boldsymbol{u}\cdot\boldsymbol{\nabla} w - f_h u &= -\partial_z p + b &&\\
\partial_t b + \boldsymbol{u}\cdot\boldsymbol{\nabla} b &= 0 && \text{buoyancy}\\
c_s^{-2}\partial_t p + \boldsymbol{\nabla}\cdot\boldsymbol{u} &= 0 && \text{continuity}
\end{aligned}
$$

- similar to non-geostrophic stability analysis of Stone (1971)

- slightly more general, more details in Thomsen et al. 2014 or Brüggemann and Eden 2014

Linear stability analysis

Linearize:

$$\boldsymbol{u} = \boldsymbol{U} + \boldsymbol{u}',\ b = B + b',\ p = P + p' \text{ with } \boldsymbol{U} = (U_1(z), U_2(z), 0)^T$$

basic state + first order pertubation equation

-> look for wave solutions:

$$u = u_0(z) \exp i(\omega t - kx - ly)$$

- eigen system, discretize and solve it numerically for given wavenumbers k and l:

$$\omega \boldsymbol{a}(z) \quad = \quad \boldsymbol{M}(z)\boldsymbol{a}(z) \qquad\qquad \boldsymbol{a}(z) = (u_0, v_0, w_0, b_0, p_0)^T$$

Linear stability analysis

eigen system, amplitude vector a(z), eigenvalue omega

$$\omega \boldsymbol{a}(z) \quad = \quad \boldsymbol{M}(z)\boldsymbol{a}(z) \qquad\qquad \boldsymbol{a}(z) = (u_0, v_0, w_0, b_0, p_0)^T$$

- imaginary part of eigenvalue -> **growth rate**

- real part of eigenvalue -> **phase velocity**

- positive growth rate -> growing waves

- **pick fastest growing wave solution**

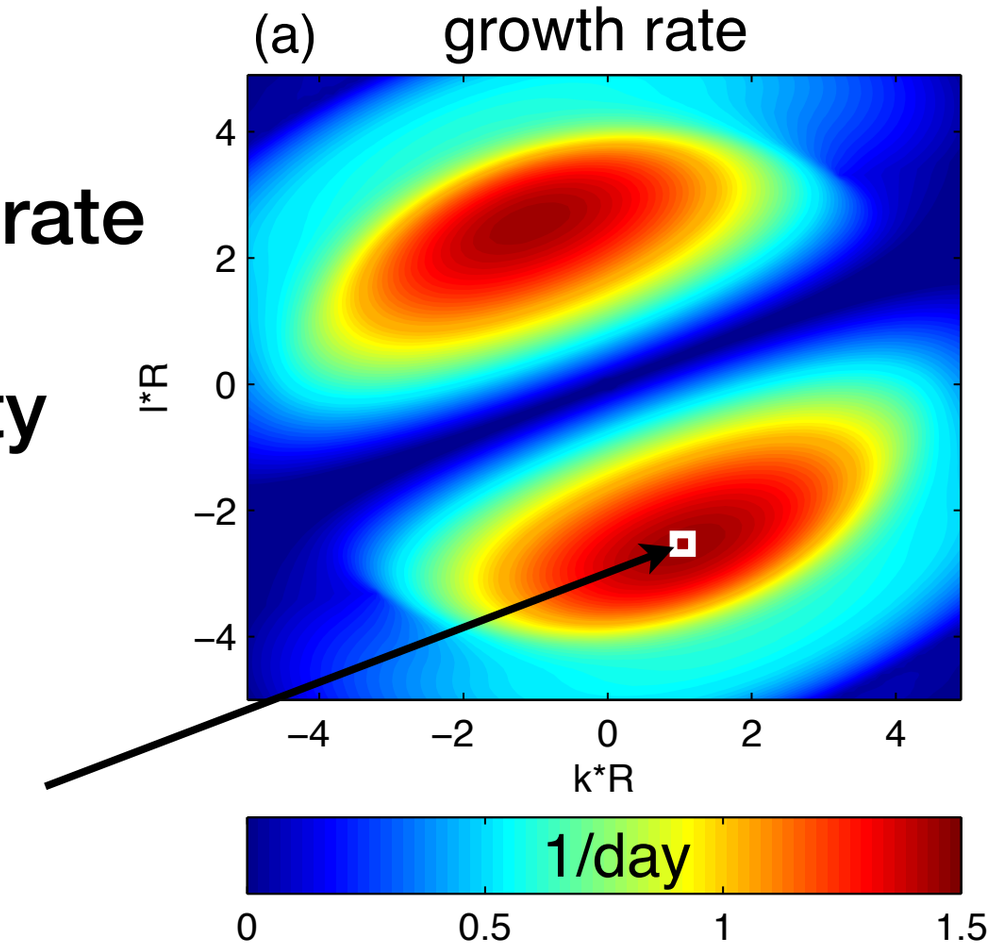

Strategy: Example profile

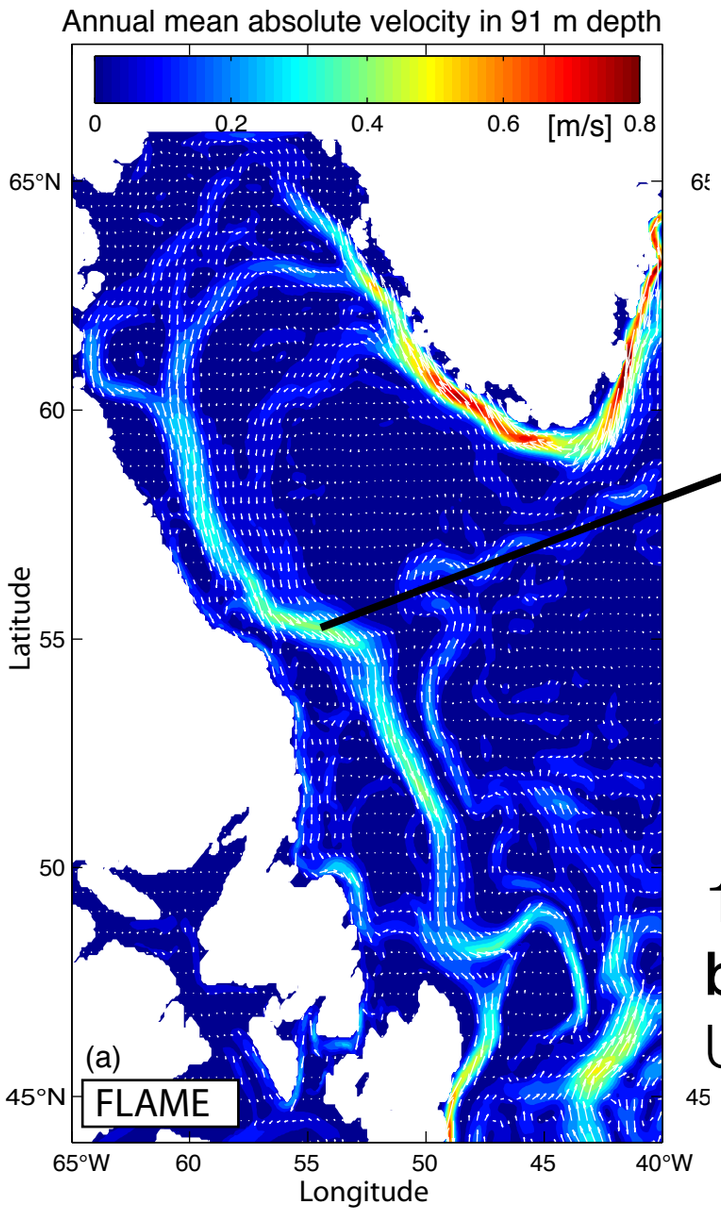

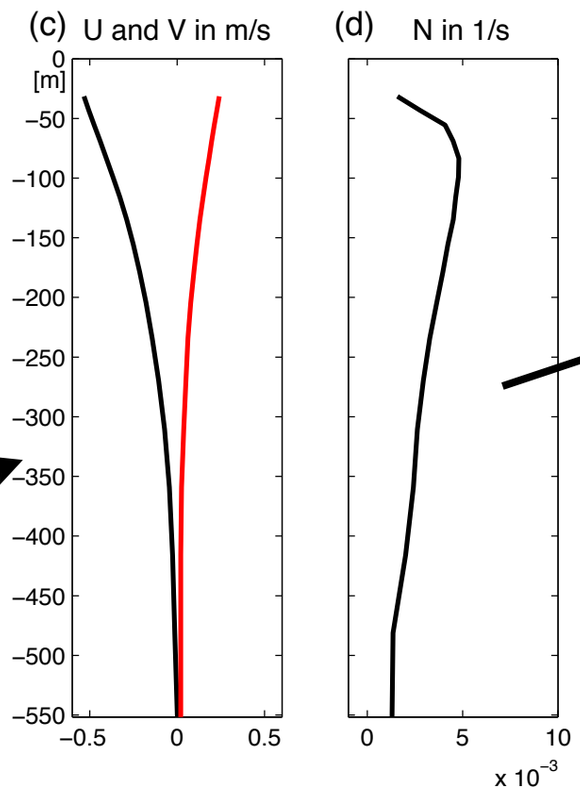

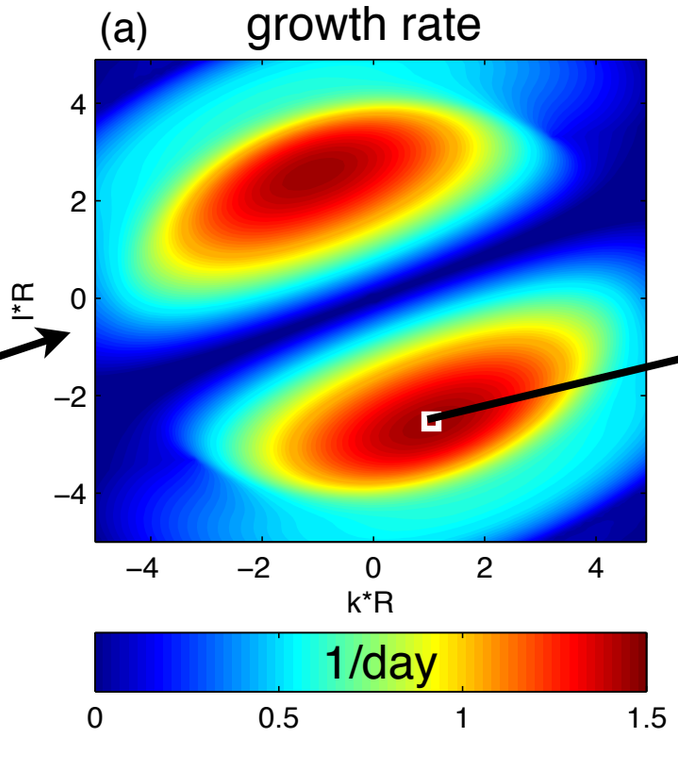

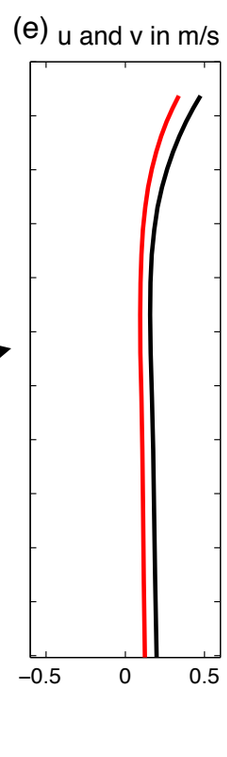

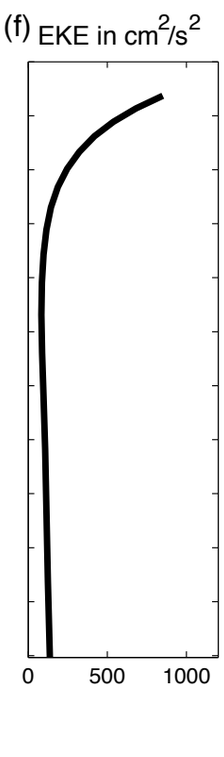

1) model delivers **basic state:** U(z), V(z), N(z)

2) LSA predicts: **growth rate** for different wave solutions

3) **maximum growth rate** -> dominant wave number

4) pertubation quantities u(z), v(z), b(z) ... and EKE(z)

- EKE scaling according to Killworth (1997), Eden (2011, 2012), Vollmer and Eden (2013)

Mapping

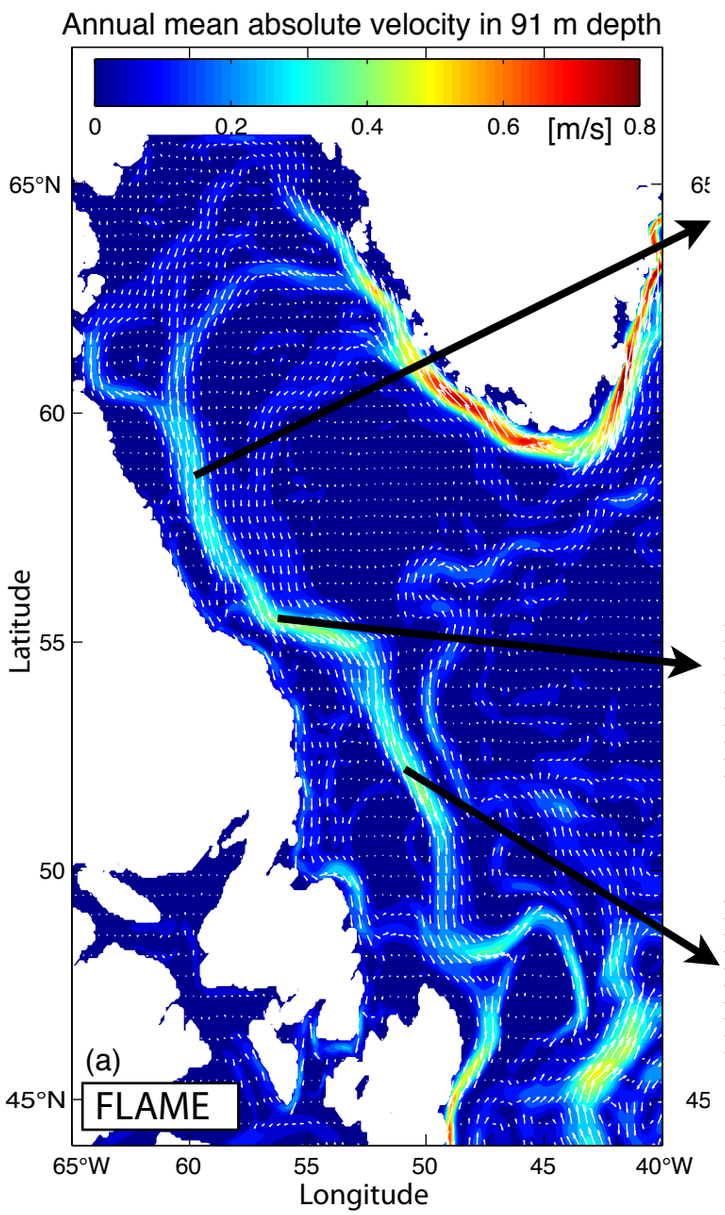

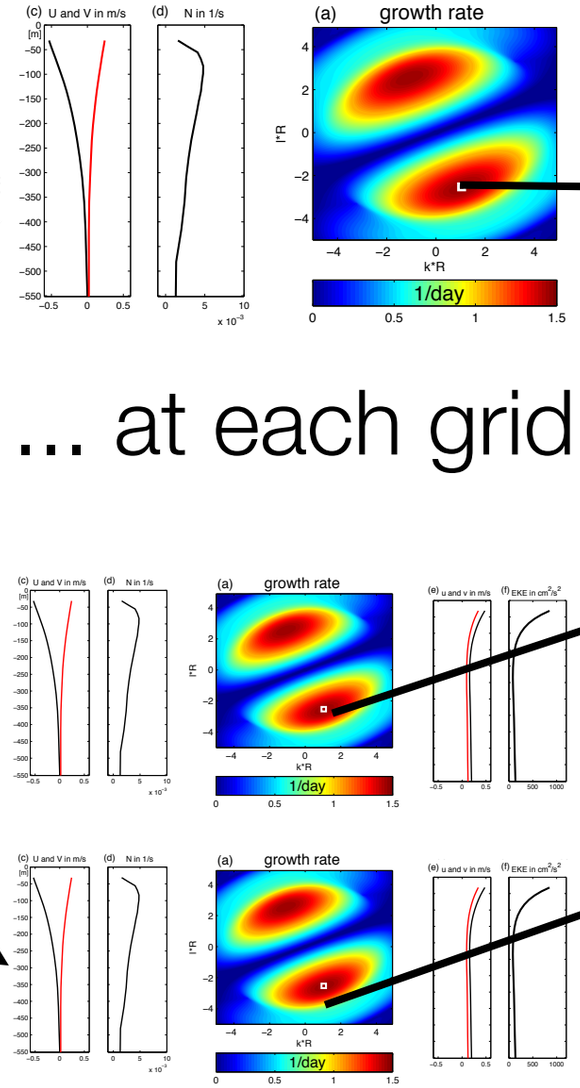

... at each grid point ...

...

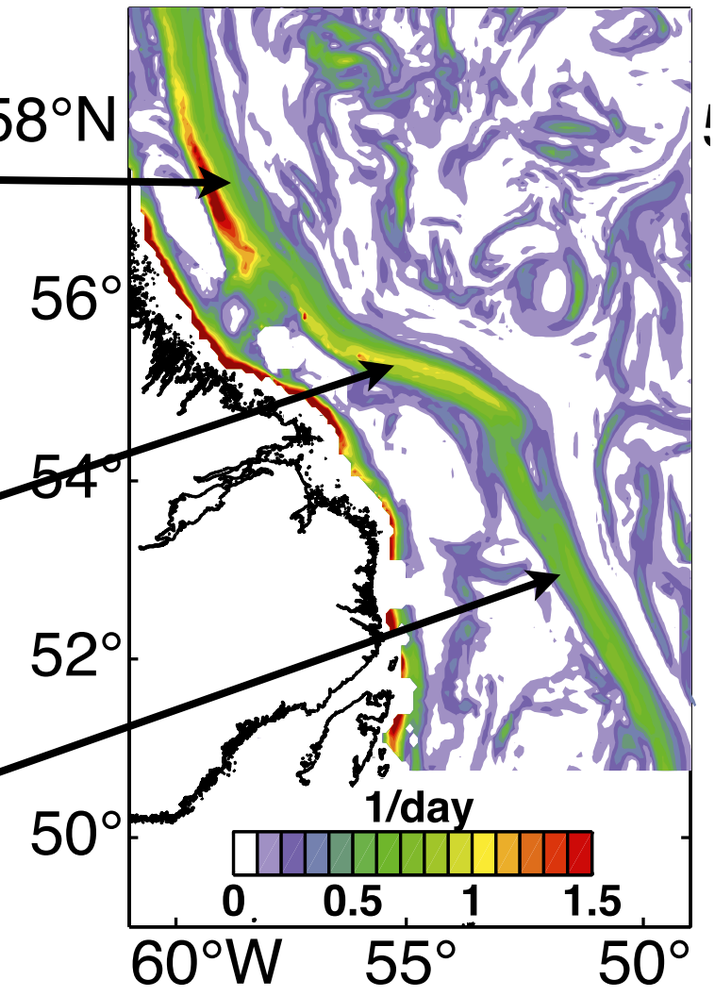

- 2D fields of growth rate, wavelength, phase speed,
- 3D fields of u',v', EKE, eddy fluxes, ...

Results
Linear stability analysis

Interior, shallow and symmetric mode

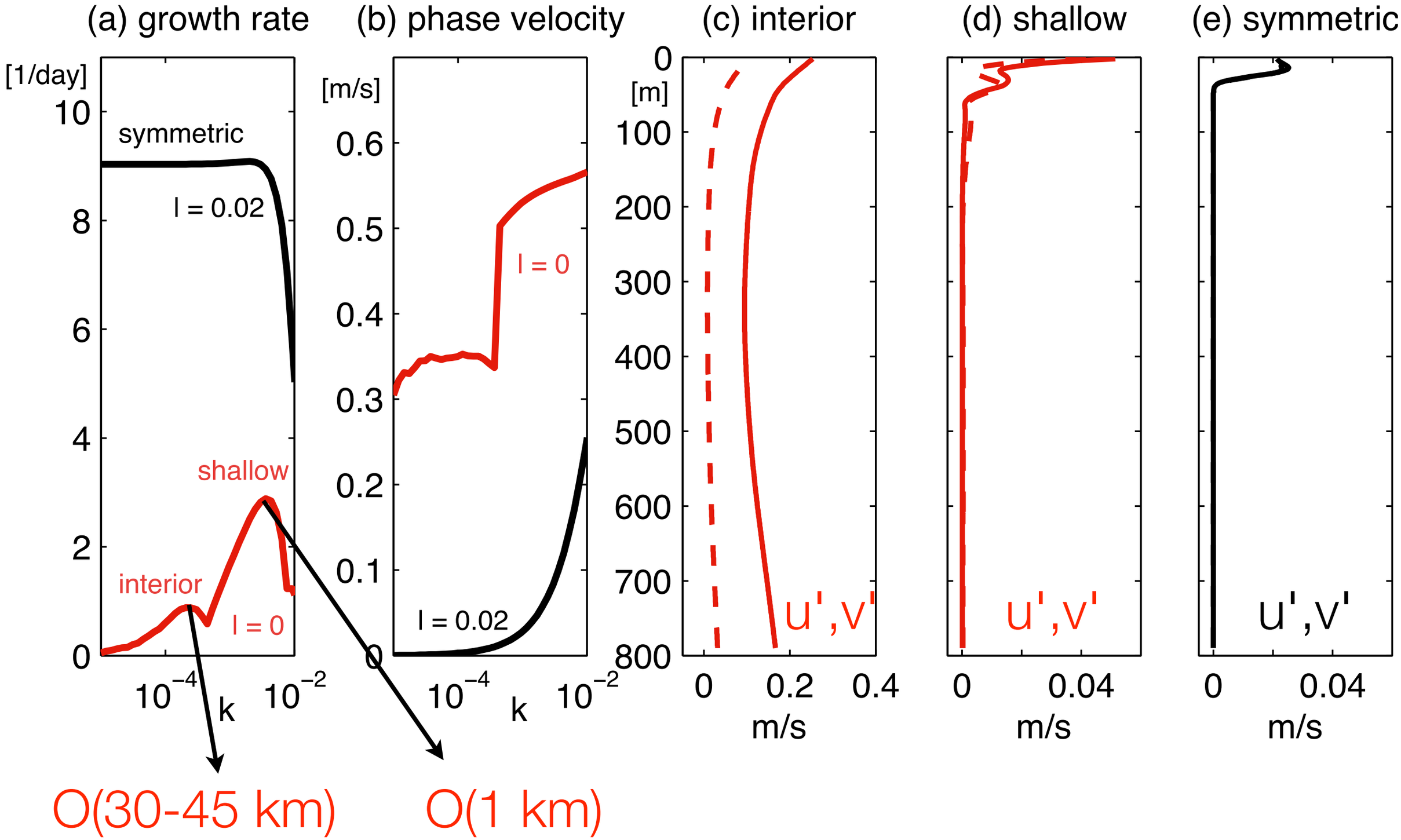

Interior mode

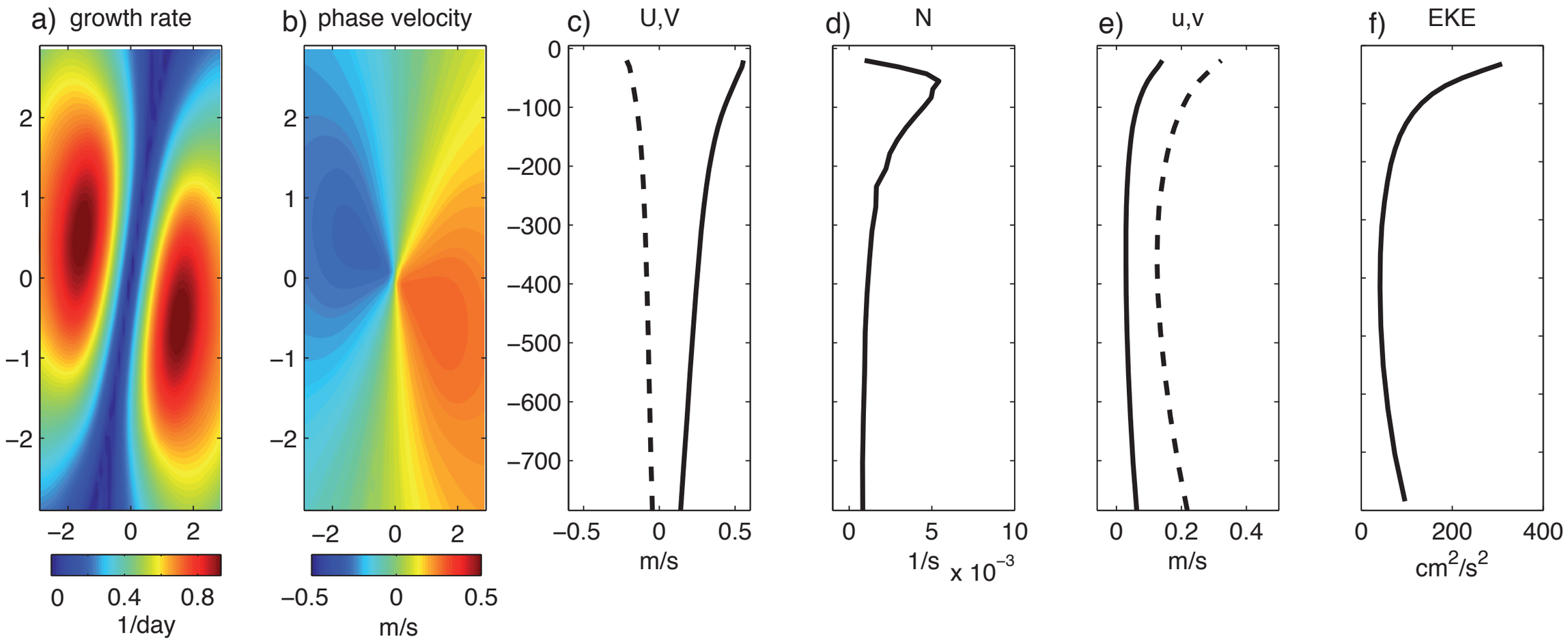

- wavelength ~ 30 - 45 km as in model
- surface intensified EKE structure as in observations and model

-> responsible for enhanced EKE in model simulations

Unstable Labrador Current in March

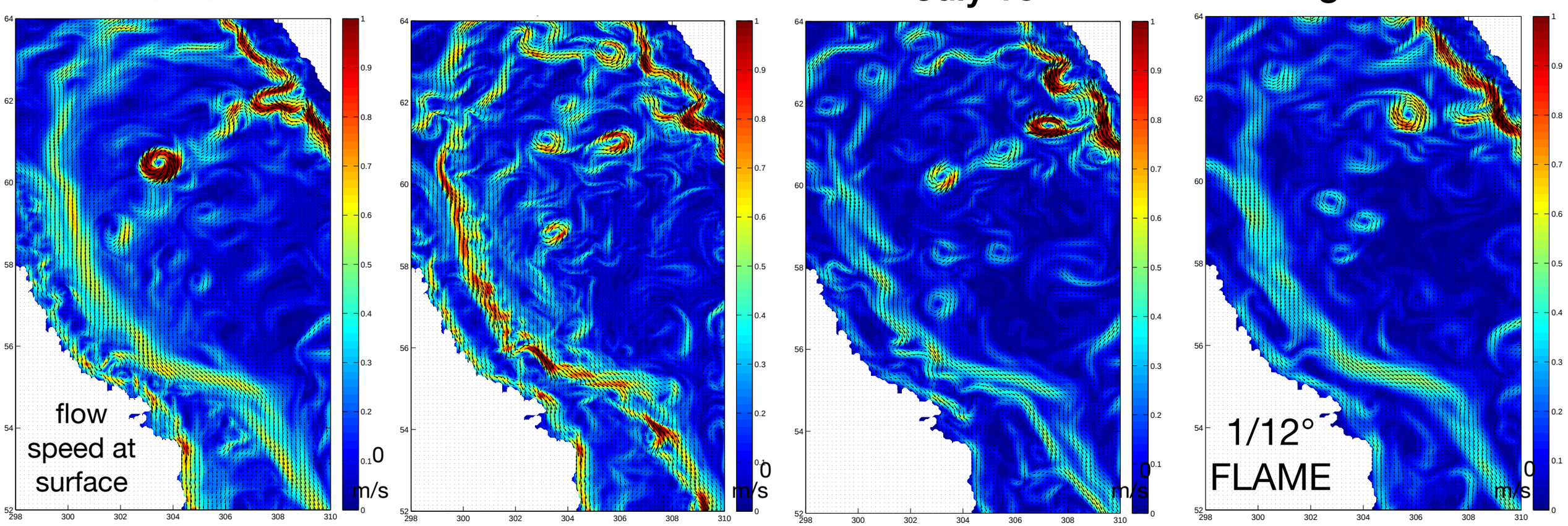

Predicted growth rates and EKE

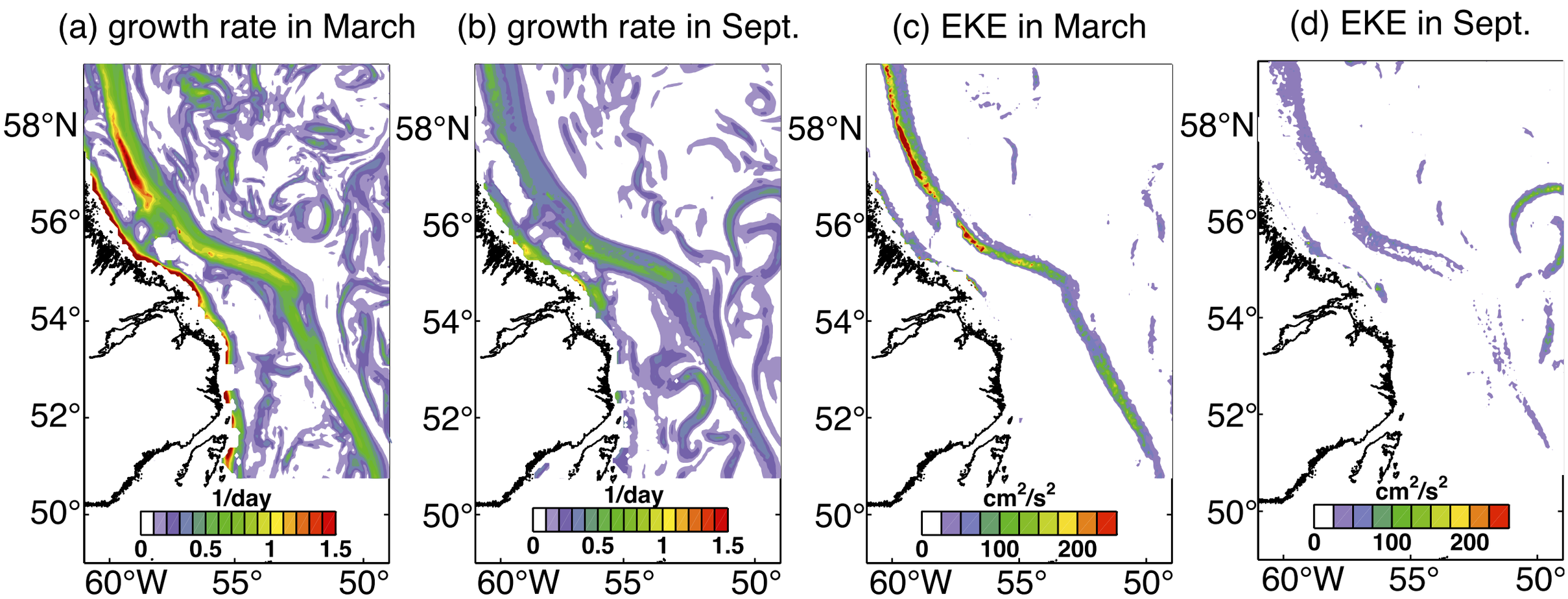

-> 3 times higher **growth rates** of **interior mode** in March compared to September

-> enhanced local EKE production in Labrador Current during March

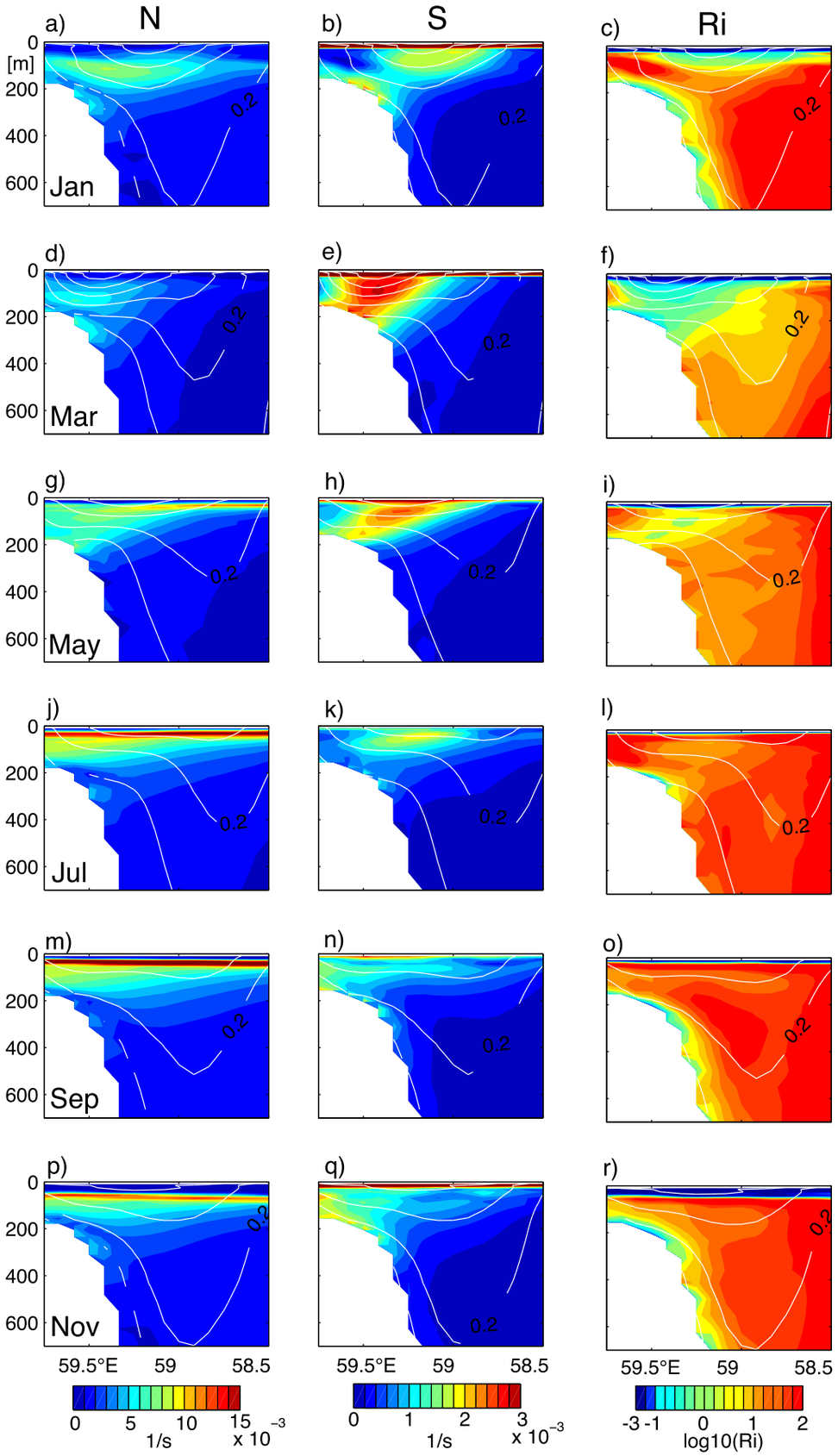

FIG. 9. Seasonal cycle of monthly-mean (left) buoyancy frequency N (s^{-1}), (middle) vertical shear (s^{-1}), and (right) the logarithm of Ri = N^2/S^2 along 57.6°N from FLAME. Also shown is the alongshore velocity component [solid white lines ($m\,s^{-1}$) with contour interval of 0.1 $m\,s^{-1}$].

Background conditions

- weak stratification
- enhanced vertical shear

-> small Richardson **numbers** (Ri < 5) in late winter

-> **growth rates** of baroclinic waves increase (Eady 1949, Stone 1970)

Back to the questions

1) Why does the Labrador Current become unstable during late winter and what kind of instability is at work?

-> interior mode is the **balanced mode of baroclinic instability at small Richardson numbers** (Stone 1970)

Back to the questions

2) How do the oceanic background conditions contribute?

-> combination of **weak stratification** and **enhanced vertical shear** result in **small Richardson numbers** in late winter

-> **local EKE production** in Labrador Current by baroclinic instability at small Richardson numbers

Baroclinic mixed layer instabilities

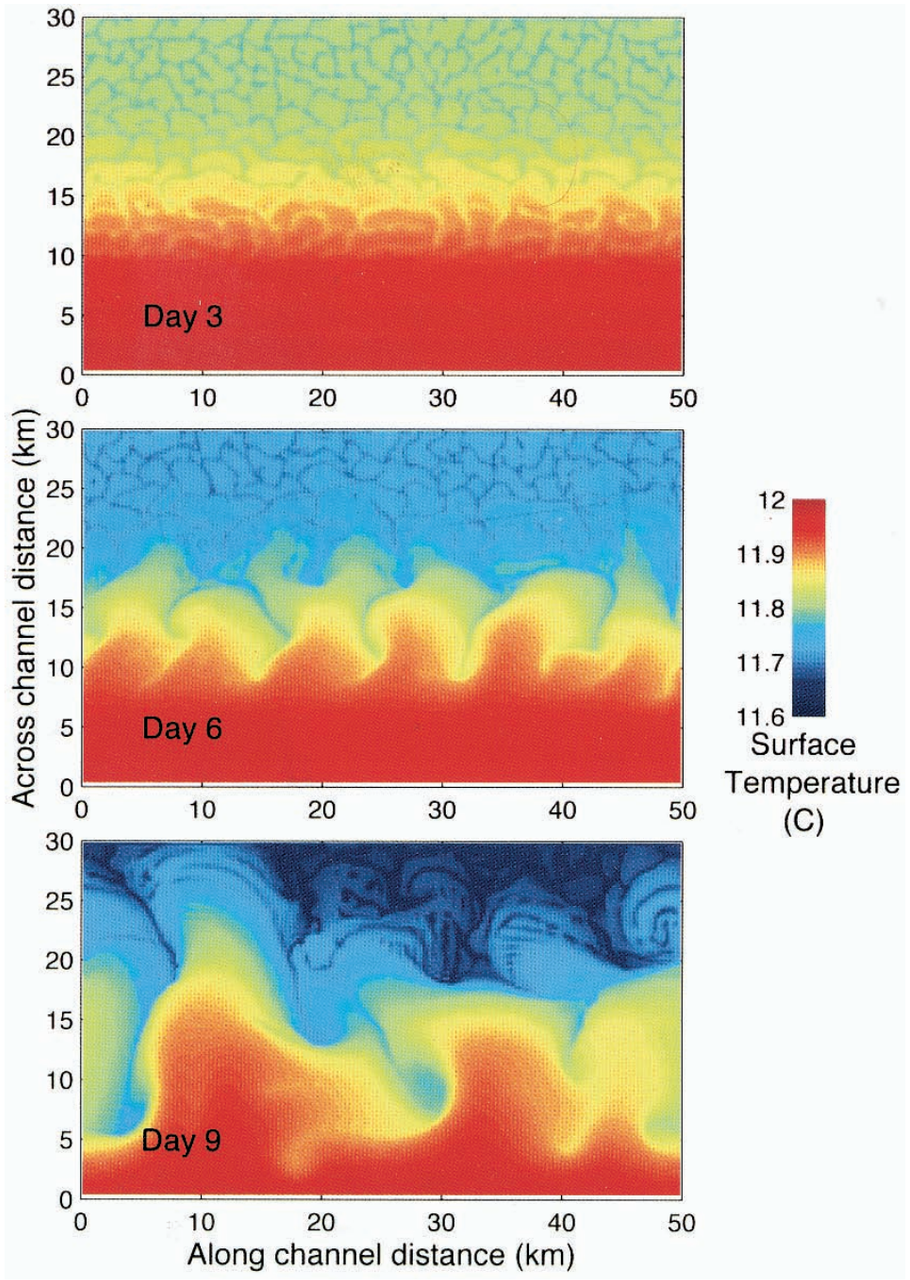

FIG. 8. The evolution of temperature at a depth of 65 m for days 3, 6, and 9 of experiment 3. The switch over from small-scale gravitational convection to finite amplitude baroclinic instability and geostrophic turbulence is clear.

Haine and Marshall 1998

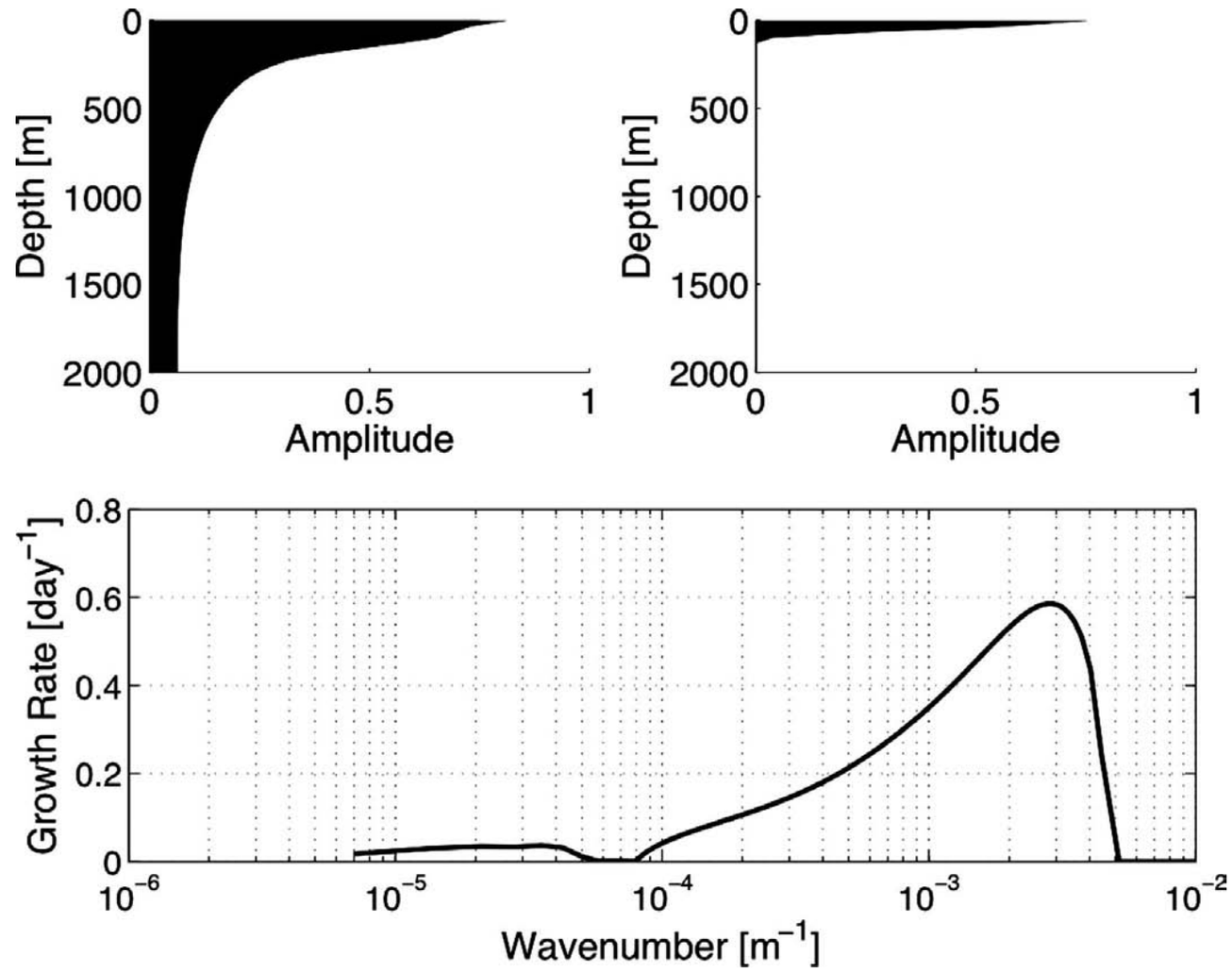

Boccaletti et al. 2007

Interior, shallow and symmetric mode

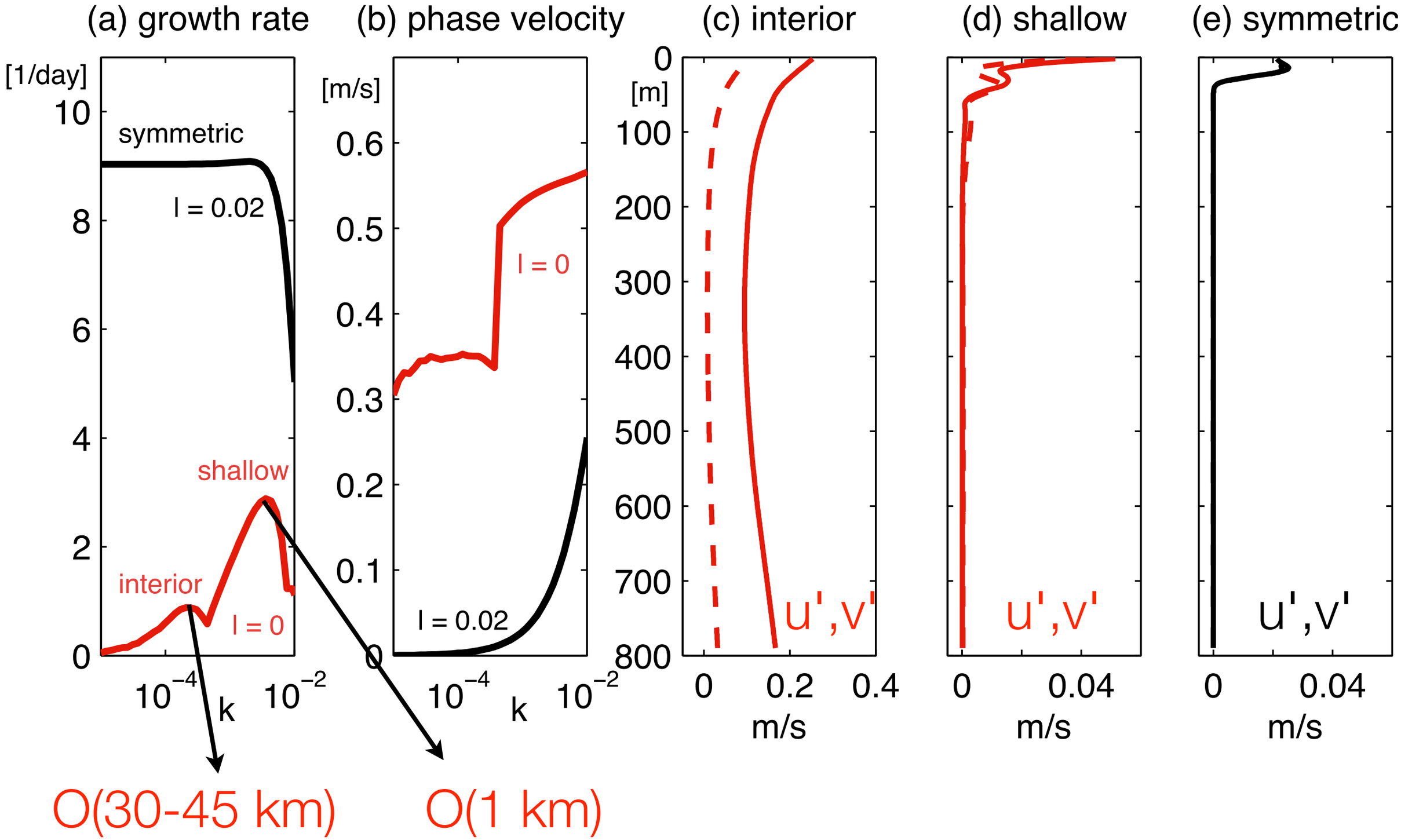

Summary

- **interior mode** L = O(30 - 45 km) has similar wavelength as first wave like disturbances in the model simulation

- **weak stratification** and **enhanced vertical shear** result in **small Richardson numbers** in the Labrador Current during late winter

-> **growth rates** of baroclinic waves **increase**

-> local EKE production in Labrador Current due to baroclinic instability at small Richardson numbers

Conclusion

- **climate** and **coarse-resolution** ocean models are not able to simulate the instability process along the Labrador Current

- frontal exchange processes might be underrepresented even in high-resolution ocean models as shallow / symmetric mode claim for even higher resolution

-> or better **parametrizations** of eddy fluxes
(e.g. predict eddy fluxes with linear stability analysis (e.g. Eden 2011, 2012, Vollmer et al. 2013)

References

Brandt, P., F. Schott, A. Funk, and C. S. Martins, Seasonal to interannual variability of the eddy field in the Labrador Sea from satellite altimetry, J. Geophys. Res., 109, C02028, doi:10.1029/2002JC001551, 2004.

Brandt et al. 2007

Lilly, Jonathan M., Peter B. Rhines, Martin Visbeck, Russ Davis, John R. N. Lazier, Friedrich Schott, David Farmer, 1999: Observing Deep Convection in the Labrador Sea during Winter 1994/95. J. Phys. Oceanogr., 29, 2065–2098.
doi: http://dx.doi.org/10.1175/1520-0485(1999)029<2065:ODCITL>2.0.CO;2

Felix, Morsdorf, Diploma Thesis, 2001

Eady, E. T. (1949), Long waves and cyclone waves, Tellus, 1(3), 33–52, doi: 10.1111/j.2153-3490.1949.tb01265.x.

Eden, C., and C. Böning (2002), Sources of eddy kinetic energy in the labrador sea, Journal of Physical Oceanography, 32(12), 3346–3363, doi:10.1175/1520- 0485(2002)032<3346:SOEKEI>2.0.CO;2.

Fischer, J., F. A. Schott, and M. Dengler (2004), Boundary circulation at the exit of the labrador sea, Journal of Physical Oceanography, 34 (7), 1548–1570, doi:10.1175/1520- 0485(2004)034<1548:BCATEO>2.0.CO;2.

Stone, P. H. (1966), On non-geostrophic baroclinic stability, Jour- nal of the Atmospheric Sciences, 23(4), 390–400, doi:10.1175/1520- 0469(1966)023<0390:ONGBS>2.0.CO;2.

Stone, P. H. (1970), On Non-Geostrophic Baroclinic Stability: Part II., Journal of Atmospheric Sciences, 27, 721–726, doi:10.1175/1520- 0469(1970)027<0721:ONGBSP>2.0.CO;2.

Stone, P. H. (1971), Baroclinic stability under non-hydrostatic conditions, Journal of Fluid Mechanics, 45(04), 659–671, doi:10.1017/S0022112071000260.

Straneo et al. 2002

Pickart et al. 1997, 2002,

Spall and Pickart 2001

Pickart and Spall 2007

Fischer et al. 2010, 2014

Rhein et al. 2015

Balanced vs. ageostrophic mode

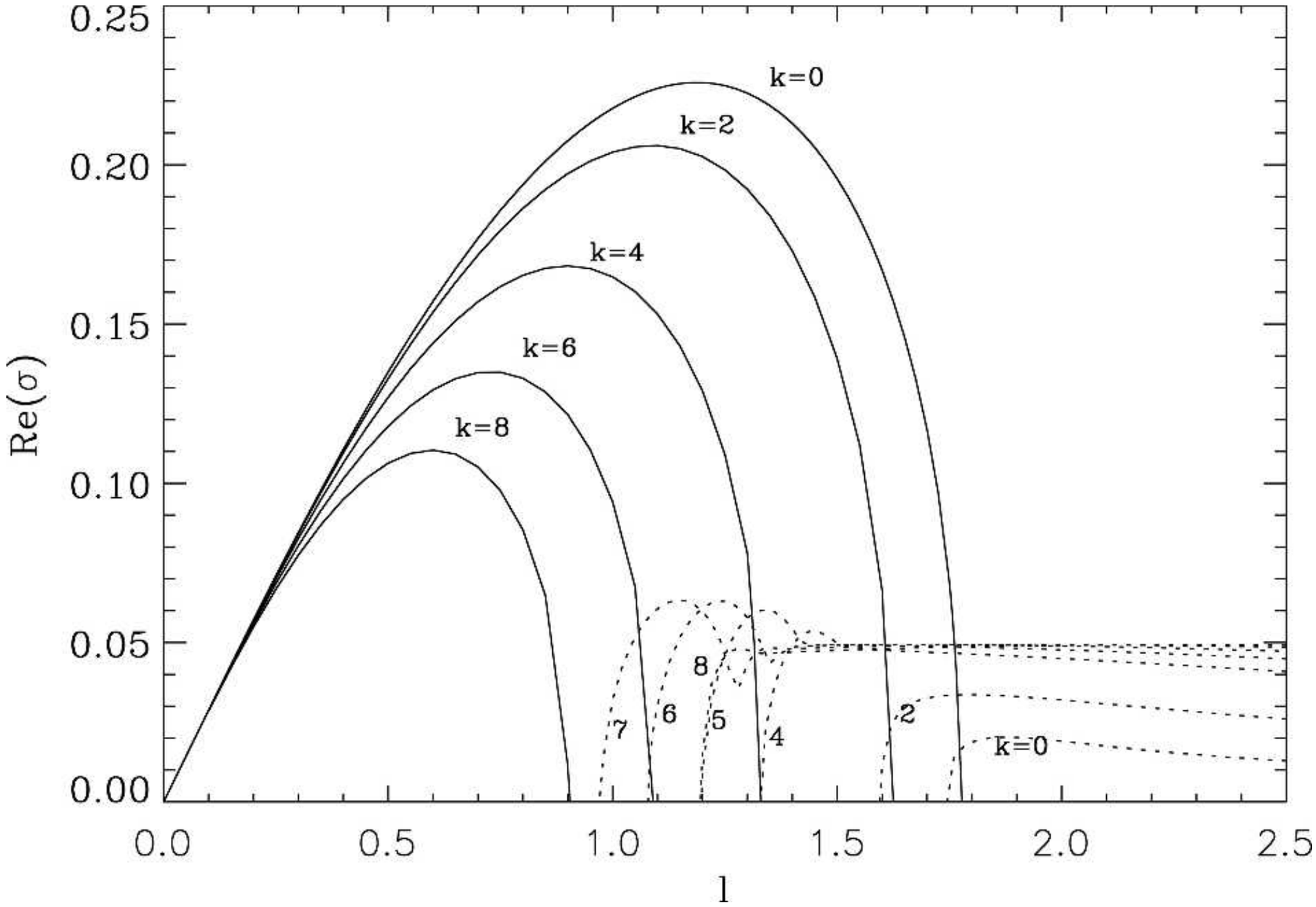

Stone 1971, Molemaker 2005

Shallow and symmetric mode

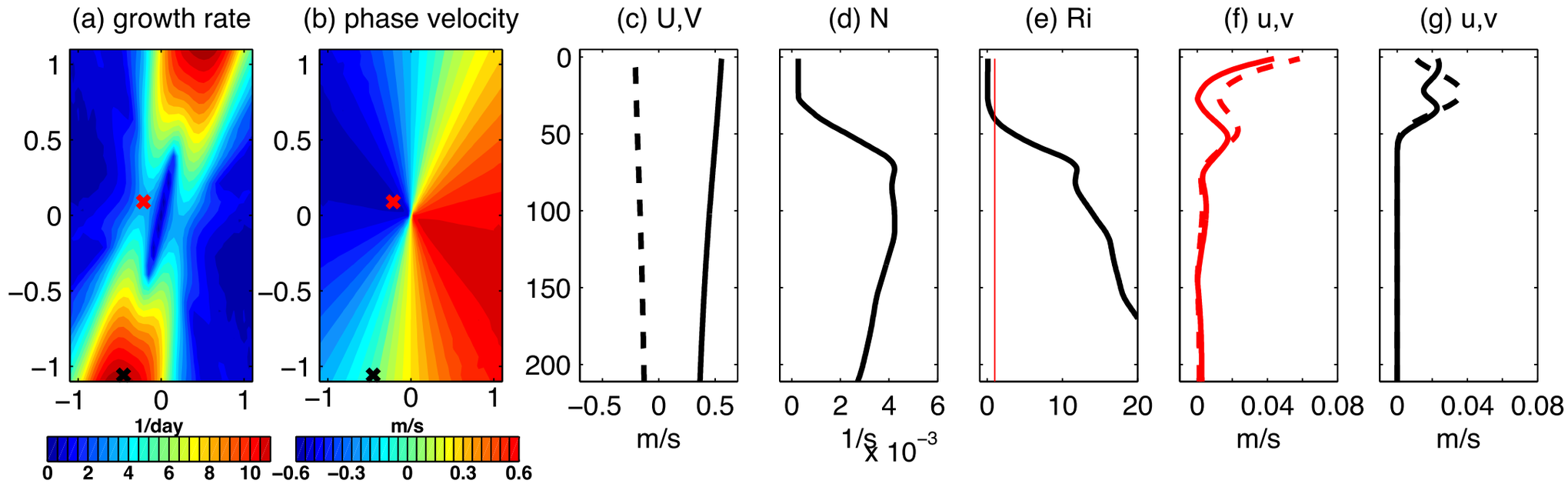

FIG. 6. The (red cross) shallow and (black cross) symmetric modes at K6 for background shear and stratification taken from January-mean values in FLAME. Shown are the (a) growth rate (day^{-1}), (b) phase velocity ($m\,s^{-1}$), (c) monthly-mean background velocity U (solid) and V (dashed) ($m\,s^{-1}$), (d) background N (s^{-1}), and (e) Ri. The red line in (e) indicates Ri = 1. (f) Velocity perturbations u (solid) and v (dashed) of the shallow mode ($m\,s^{-1}$) and (g) the corresponding variables for the symmetric mode. The wavenumbers in (a),(b) are scaled with the mixed layer Rossby radius (see text for definition). The U and V at velocity grid points closest to the mooring positions and N^2 interpolated on these points are taken as background values.

- **shallow mode** with lateral scales of O (1 km)
-> submesoscale variability (Boccaleti ...
- symmetric instabilities arise at Ri < 1 (Haine ..., Straneo et al. 2002)
- both modes remain unresolved in 1/12° simulations